Journal of Materials Chemistry C

The luminescent sensing profiles based on anion-responsive lanthanide(III) quinolinecarboxylate materials: solid-state structures, photophysical properties, and anionic species recognition

Journal:	*Journal of Materials Chemistry C*
Manuscript ID:	TC-ART-10-2014-002369.R1
Article Type:	Paper
Date Submitted by the Author:	18-Dec-2014

Complete List of Authors:	Xu, Wentao; Fujian Institute of Research on the Structure of Matter, Chinese Academy of Sciences, Key Laboratory of Optoelectronic Materials Chemistry and Physics Zhou, Youfu; Fujian Institute of Research on the Structure of Matter, Chinese Academy of Sciences, Key Laboratory of Optoelectronic Materials Chemistry and Physics Huang, Decai; Fujian Institute of Research on the Structure of Matter, Chinese Academy of Sciences, Key Laboratory of Optoelectronic Materials Chemistry and Physics Su, Mingyi; Fujian Institute of Research on the Structure of Matter, Chinese Academy of Sciences, Key Laboratory of Optoelectronic Materials Chemistry and Physics; University of the Chinese Academy of Sciences, Wang, Kun; Fujian Institute of Research on the Structure of Matter, Chinese Academy of Sciences, Key Laboratory of Optoelectronic Materials Chemistry and Physics; University of the Chinese Academy of Sciences, Xiang, Ming; Fujian Institute of Research on the Structure of Matter, Chinese Academy of Sciences, Key Laboratory of Optoelectronic Materials Chemistry and Physics; University of the Chinese Academy of Sciences, Hong, Maochun; Fujian Institute of Research on the Structure of Matter,, State Key Laboratory of Structural Chemistry

Cite this: DOI: 10.1039/c0xx00000x

www.rsc.org/xxxxxx

ARTICLE TYPE

The luminescent sensing profiles based on anion-responsive lanthanide(III) quinolinecarboxylate materials: solid-state structures, photophysical properties, and anionic species recognition

Wentao Xu,[a] Youfu Zhou,*[a] Decai Huang,[a] Mingyi Su,[ab] Kun Wang,[ab] Ming Xiang[ab] and Maochun Hong[a]

Received (in XXX, XXX) Xth XXXXXXXXX 20XX, Accepted Xth XXXXXXXXX 20XX
DOI: 10.1039/b000000x

Lanthanide complexes based on quinoline-based carboxylate ligand 2-phenyl-4-quinolinecarboxylic acid (PQC), namely $\mathbf{Ln_2PQC_6}$ (Ln = La^{3+}, Pr^{3+}, Nd^{3+}, Sm^{3+} and Eu^{3+}) were synthesized by convenient solvothermal reaction, and related crystal structures have been determined. These complexes are isostructural and feature a discrete dinuclear moiety, where solvent molecules act as coligands and the Ln^{3+} centre exhibits distorted tricapped trigonal prism geometry. By the introduction of PQC ligand, the europium sample $\mathbf{Eu_2PQC_6}$ **(5)** showing intense red emission in solid state and solution, with both of the replaceable coordination environment and potential hydrogen-bonding-accepting site, can be explored as a luminescent probe for sensing various anions. Among the tested ions (F^-, Cl^-, Br^-, I^-, NO_3^-, ClO_4^-, SCN^-, HCO_3^-, HSO_4^- and $H_2PO_4^-$), HSO_4^- and $H_2PO_4^-$ possess strong response in the Eu^{3+} emitting behaviour leading to a unique quenching with a low detection limit of 15.3 and 8.3 nM respectively, and a quick respond time less than 30s. The different recognition mechanisms for two anions including O-H---N hydrogen bonding and metal coordination modes have been proposed, supported by UV-vis, fluorescence spectroscopy, nuclear magnetic resonance (NMR) and X-ray photoelectron spectroscopy (XPS) measurements. In addition, density functional theory (DFT) calculations were carried out to vindicate two recognition mechanisms of $\mathbf{Eu_2PQC_6}$ in depth. As an extended research, $\mathbf{Eu_2PQC_6}$ interaction with the nucleoside phosphates adenosine triphosphate (ATP), adenosine diphosphate (ADP) and adenosine monophosphate (AMP) in mixed aqueous solution has been investigated, which can acts as a special luminescent sensor for all three phosphates. The strong quenching by ADP (99.5%), has been ascribed to strong bonding affinity (log K_a = 5.99) based on electrostatic attraction and steric effect.

Introduction

Anions play fundamental roles in biology, as well as in environmental and industrial application including physiological processes to life, medicine, molecular assembly, catalysis, and host–guest chemistry.[1-4] Among various anions, hydrogen sulfate ion (HSO_4^-) is of particular importance owing to established role in industry and biology.[5] HSO_4^- existing in nuclear fuel waste could ionize to toxic sulfate ion (SO_4^{2-}), causing irritation of the skin, eyes and respiratory. In addition, the phosphate ions are ubiquitous in biological systems possessing a unique importance in genes and metabolic pathways with a normal concentration of 3.5 mg dL^{-1}.[6] Nucleoside phosphates play a vital role in DNA replication and transcription, while triphosphate (ATP) cleaved into diphosphate (ADP), monophosphate (AMP), orthophosphate and pyrophosphate acts as a universal energy source. ATP deficiency may result in ischemia, Parkinson's disease and hypoglycaemia.[7] Excess phosphate causes hyperphosphatemia leading to severe cardiovascular and kidney problems.[8]

Therefore, studies on the recognition, detection, and extraction of such environmentally and biologically significant anions have gained great interest.[9] Motivation behind the research lying in an immense amount of implications insures that much effort is directed towards the development of molecular system for anion probe. Common anions are larger and more diffuse charged than cations, which is challenge to predetermine and synthesize receptors to effectively compete with solvent molecules for anion binding of high affinity.[9a,e] Several examples of sensors for hydrogen sulfate and phosphate have been reported,[10,11] where the main design strategies are employed based on supramolecular recognition. Many aforementioned anion receptors endowed with hydrogen-bonding-donating moieties, like amide, urea, thiourea, imidazole and pyrrole, have been coupled with organic fluorescence signalling molecules to construct fluorometric anion probes.[12-16] However, most of the reported organic molecules cannot surmount their limitations, suffering from complicated synthetic procedures, short fluorescence lifetime fell in the range of nano-seconds, narrow energy gap, and interference caused by auto-fluorescence from surrounding biological environments or light scattering.[17]

Recently, major research interest has been focused on fluorescent sensors based on lanthanide complex, taking

advantage of sharp emission lines arising from characteristic 4f electronic transitions, and the analyte-induced hyperfine energy transfer or change of coordination environment mechanism to offer considerable virtues over typical luminescent complexes.[18] Thanks to high luminous efficiency, large Stokes shift and long luminescence lifetime, lanthanide complexes, which allow for time-resolved fluorescence (TRF) measurements, have significant potential for applications.

Inspired by the properties of both above systems, we try to bring in quinoline moiety as hydrogen-bonding-accepting site into lanthanide complex. Different from the typical N–H---X hydrogen-bond groups, which elicit a similar receptor affinity or sensor response with only moderate selectivity for the hydrogenous and hydrogenous-free anions (i.e., F^- and HSO_4^-),[19] besides the valuable antenna effect for sensitizing Ln^{3+} emission, quinoline has peculiar O–H---N hydrogen-bond interaction with given hydrogenous anion to improve the selectivity, which is not much explored to date. In addition, direct coordination of the anion (ie., $H_2PO_4^-$) to the lanthanide ion is typically anticipated, so in solution, displacement of coordinate solvent molecules or ligands results in changes of local coordination environment, leading to detectable luminescent signal. Therefore integrating hydrogen-bond moiety and lanthanide coordination site within a single structure, the quinoline-based lanthanide luminescent sensor can distinguish anions by different electrostatic bonding natures simultaneously.

Toward this end, 2-phenyl-4-quinolinecarboxylic acid (PQC), incorporating carboxylate and quinoline groups, which has been proven to be a versatile ligand for construction of lanthanide complex,[20] is introduced to build novel luminescent sensor system. Since the "hard acid" of Ln^{3+} is not affinitive to the "soft base" N atom, when PQC reacts with Ln^{3+}, the quinolyl N atoms are always uncoordinated.[20,21] These preserved N sites could interact with demanded ion through O–H---N hydrogen-bond interaction leading to luminescence intensity changes of Ln^{3+} centre. Herein, a series of binary PQC based lanthanide complexes **Ln_2PQC_6**, (Ln = La (**1**), Pr (**2**), Nd (**3**), Sm (**4**) and Eu (**5**)) have been designed and synthesized for their fluorescent properties, in which **5** was the only complex obtained as strong red-emitting luminescent material. Thus, **5** as fluorescent probe for detecting HSO_4^- , $H_2PO_4^-$ and extending to nucleoside phosphates has been investigated first time. The sensitivity, selectivity and different recognition mechanisms for such anions have also been elucidated in detail. To the best of our knowledge, this is the first report that focuses on the luminescent behavior concerning different anion stimulation by quinoline ring-based lanthanide luminescence probes. This novel system possessing both of weak (hydrogen-bond) and strong (coordination) interactions for the easy detection of various anions, has provided direct and quantitative information on the performance of lanthanide fluorescent sensor.

Experimental section

Materials and Characterization

PQC (2-phenyl-4-quinolinecarboxylic acid) was purchased from Alfa Aesar; sodium and tetrabutylammonium (TBA) salts, (NaX or [TBA]X, X = F^-, Cl^-, Br^-, I^-, NO_3^-, ClO_4^-, SCN^-, HCO_3^-, HSO_4^- and $H_2PO_4^-$) were purchased either from Aladdin or Alfa Aesar; triphosphate (ATP), diphosphate (ADP) and monophosphate (AMP) were purchased from Adamas; the dimethylsulfoxid-d_6 (DMSO-d_6) for ^{1}H-NMR experiments was purchased from Sigma-Aldrich. All other solvents and reagents were of analytical grade and used as received without further purification.

Elemental analysis for C, H, N were carried out on a Vario EL 3+ elemental analyzer. Infrared spectra (IR) were recorded with KBr pellets on a PerkinElmer Spectrum One FT-IR spectrometer in the range of 4000−400 cm^{-1}. Thermal gravimetric analysis (TGA) were performed using NETZSCH STA 449C instrument. The powder X-ray diffraction (PXRD) patterns were collected using a diffractometer RIGAKU D/MAX2500 with Cu Kα radiation (λ=1.5406Å). X-ray photoelectron spectroscopy (XPS) measurements were performed on ESCALAB 250Xi. ^{1}H NMR spectra were recorded on an AVANCE 3+ spectrometer in DMSO-d_6 with TMS as an internal standard. Mass spectra are recorded with a DECAX-30000 LCQ Deca XP ion trap mass spectrometer in the ESI mode. The UV−vis absorption spectra were collected on a Lambda-900 instrument from the Perkin−Elmer Corporation. Emission and excitation spectra were recorded on a Horiba Jobin−Yvon Fluorolog-3 spectrophotometer analyzer with the slit widths at 2.0 or 4.0 nm. Quantum yield and lifetime were performed on an Edinburgh Instruments model FLS920 spectrofluorometer equipped with both a continuous (450 W) 124 xenon lamp and a pulse xenon lamp.

Preparation of single crystals of Ln_2PQC_6

A mixture of $Ln(NO_3)_3{\cdot}6H_2O$ (0.1mmol) (Ln = La^{3+}, Pr^{3+}, Nd^{3+}, Sm^{3+} and Eu^{3+}), PQC (0.3 mmol) and enthanol (EtOH) (10 mL) was sealed in a 23 mL Teflon-lined stainless steel autoclave under autogenous pressure at 100 ˚C for 4 days. After cooling to room temperature at a rate of 40˚C/h, the clear yellow solution was transferred to 25 mL quartz glass vial with cap, under autogenous pressure at 80 ˚C for another 3 days, and then allowed to cool to room temperature slowly at a rate of 3˚C/h. The yellow prism-shaped crystals were obtained by filtration, washed with ethanol and dried in air.

La_2PQC_6 (**1**). Yield: 48% (based on La^{3+}). Elemental analysis (%). Anal. Calcd for $C_{54}H_{48}EuN_3O_9$: C, 63.46; H, 4.73; N, 4.11. Found: C, 63.52; H, 4.82; N, 4.20. IR (KBr, cm^{-1}): 3401(b), 2025(m), 1618(s), 1547(s), 1391(s), 1321(m), 1238(m), 772(w).

Pr_2PQC_6 (**2**). Yield: 45% (based on Pr^{3+}). Elemental analysis (%). Anal. Calcd for $C_{54}H_{48}EuN_3O_9$: C, 63.33; H, 4.72; N, 4.10. Found: C, 63.56; H, 4.66; N, 4.13. IR (KBr, cm^{-1}): 3386(b), 2026(m), 1615(s), 1540(s), 1392(s), 1310(m), 1240(m), 768(m).

Nd_2PQC_6 (**3**). Yield: 32% (based on Nd^{3+}). Elemental analysis (%).Anal. Calcd for $C_{54}H_{48}EuN_3O_9$: C, 63.11; H, 4.70; N, 4.09. Found: C, 62.61; H, 4.58; N, 4.18. IR (KBr, cm^{-1}): 3397(b), 2027(w), 1608(s), 1533(s), 1396(s), 1323(m), 1236(w), 772(m).

Sm_2PQC_6 (**4**). Yield: 51% (based on Sm^{3+}). Elemental analysis(%).Anal. Calcd for $C_{54}H_{48}EuN_3O_9$: C, 62.78; H, 4.68; N, 4.07. Found: C, 61.82; H, 4.46; N, 4.09. IR (KBr, cm^{-1}): 3355(b), 2020(m), 1617(m), 1543(s), 1392(s), 1327(m), 1236(w), 771(m).

Eu_2PQC_6 (**5**). Yield: 45% (based on Eu^{3+}). Elemental analysis (%). Anal. Calcd for $C_{54}H_{48}EuN_3O_9$: C, 62.66; H, 4.67; N, 4.06. Found: C, 61.73; H, 4.52; N, 4.11. IR (KBr, cm^{-1}): 3356(b), 2012(m), 1608 (m), 1533(s), 1395(s), 1306(m), 1236(w), 764(m).

General methods

Unless otherwise stated, the temperature was kept constant throughout the measurements at 298 K. The test solutions were prepared by placing in quartz cells with a 1 cm path length and a fixed volume of 2.7 mL. The resulting solution was shaken for 5 min well before record. The LOD of the $\mathbf{Eu_2PQC_6}$ for the analysis of anions was determined from the titration experiment following the reported method from a plot of changes in fluorescence intensity as a function of the concentration of the added ions.[22] To determine the S/N ratio, the fluorescence intensity of $\mathbf{Eu_2PQC_6}$ as blank sample without anions was measured 10 times and the standard deviation of the blank measurements was determined. The detection was calculated as three times the standard deviation from the blank measurement divided by the slope of calibration plot between ion concentration and fluorescence intensity. The LOD was following equation: LOD = 3σ/S, where σ is the standard deviation; S is the slope of the calibration curve. All the calculations were implemented in Gaussian 09 program.[23] The density functional theory (DFT) method at the hybrid Becke three-parameter Lee-Yang-Parr (B3LYP)[24] functional level was used to study the interaction between europium ion and $HSO_4^-/H_2PO_4^-$. In these calculations, the energy-consistent pseudopotential of the Stuttgart/Cologne group ECP52MWB was used to describe the inner 52 electrons of europium atoms, while its associated basis set was employed for the remaining outer electrons.[25] And all-electron basis set of 6-31G** was used for non-metal H, C, N, O, P, and S atoms. The dispersion corrected B3LYP level of theory (B3LYP-D3)[26] was used to carry out the calculation for hydrogen-bonding-interaction. During these calculation processes, the symmetry restriction of structures were not considered, the convergent values of maximum force, root-mean-square (RMS) force, maximum displacement, and RMS displacement were set by default. Then, the energies were obtained in the corresponding optimized results of investigated compounds.

Single crystal structure determination

Single crystal data for **2, 4, 5** were collected on a SuperNova CCD diffractometer with graphite-monochromated Cu Kα radiation (λ= 1.54178 Å) by using the ω-2θ scan method at 100.00(15) K, and **3** were collected on Saturn 70 CCD diffractometer with graphite-monochromated Mo Kα radiation (λ= 0.71073 Å) at 293(2) K. All of the structures were solved with direct methods and refined on F^2 with full-matrix least-squares methods using SHELX-97 program.[27] All non-hydrogen atoms were refined anisotropically. The hydrogen atoms are located geometrically and treated as a riding model. CCDC 1026999-1027002 (**2**−**5**), contain the supplementary crystallographic data for this paper.

Results and discussion

Synthesis

All the yellowish crystalline **1**–**5** have been synthesized by reaction of lanthanide nitrates and the PQC ligands in ethanol solution under two-step solvothermal conditions. It is noteworthy that despite all our efforts, we were not successful in gaining good sample of **1** for single crystal X-ray diffraction. However, the cell parameters with a = 12.1 Å, b = 12.9 Å, c = 15.9 Å, and α = 87.5 °, β = 73.8 °, γ = 83.4 °, were closed to those of **2**–**5**, so this result combined with the elements, IR and PXRD analysis indicates that **1**–**5** are isostructural. On the contrary, the isostructures of other heavy Ln^{3+} ions were not available, ascribed to the effect of lanthanide contraction hypothetically. Light Ln^{3+} ions with larger size are more suitable to form nigh or ten coordinated numbers than that of smaller heavy ones,[28] so this molecular model would not be capable of encapsulating all of the lanthanide ions, independently of their varying sizes.

Single crystal X-ray analysis

X-ray diffraction indicates that **1**−**5** with yellowy rhombic crystals are isomorphic, the summary of crystallographic data and structural refinements are listed in Table S1† and S2†. So as a representative, the crystal structure of **5** is employed to be discussed in detail. The single-crystal X-ray analysis reveals that **5** crystallizing in the triclinic system and space group P-1, features a discrete dinuclear structure. The asymmetric unit of **5** contains half of the dinuclear unit, consisting of one crystallographically independent Eu^{3+} ion, three PQC^- ligands, two coordinated EtOH molecules, and one free EtOH molecule (Fig. S1†). Each Eu^{3+} centre is coordinated by nine oxygen atoms, including seven carboxylic oxygen atoms from three PQC^- ligands, and two oxygen atoms from two terminal EtOH molecules, respectively. As showed in Fig. 1, Eu1 and its corresponding centrosymmetric generated atom Eu1A (symmetry code A= 1-x, 1-y, -z) are joined by two bidentate bridged carboxylic groups to form a dinuclear twisty rectangular plate-like unit, with the separation of Eu···Eu being 4.048(18) Å. As a result, the coordination geometry around the metal centre can be described as distorted tricapped trigonal prism and the PQC ligands here exhibit bidentate chelating, bidentate and tridentate bridging coordination modes, respectively. The dinuclear unit is further connected by four adjacent ones to form a 3D metal-organic supramolecular framework by the π···π interactions in face-to-face mode (Fig. S2†). The dinuclear formation in ethanol solution has also been confirmed by ESI-MS spectrum with intense peaks at m/z = 1070.6, assignable to negatively charged species [$\mathbf{Eu_2PQC_6}$+4H_2O]/2 (Fig. S3†).

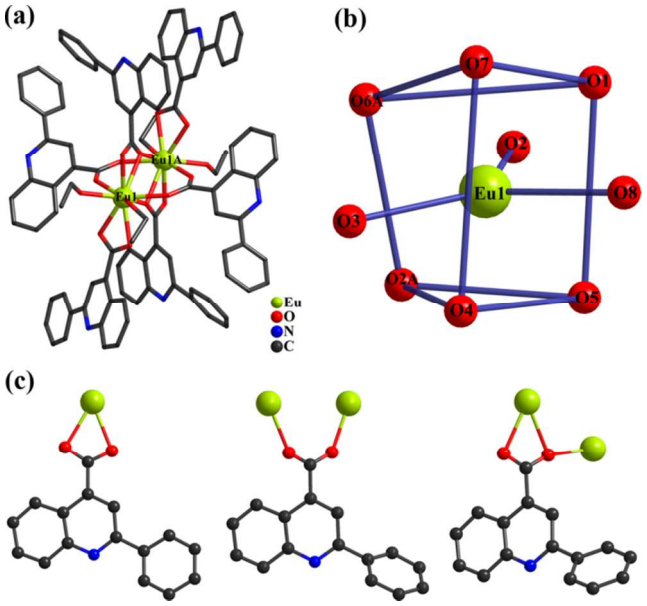

Fig. 1 (a) Structure of dinuclear unit. (b) Coordination geometry of Eu^{3+} centre. (c) Coordination modes of PQC ligand.

IR spectroscopy, thermal gravimetric analysis and powder X-ray diffraction

The IR spectra of complex **1**−**5** have many similar features corresponding to the common groups; thus, only the spectra of **5** in solid and EtOH−DMSO solution will be discussed (Fig. S4†). For solid **5**, the broad absorption bands in the range of 3050−3560 cm^{-1} are due to the aromatic C-H stretching vibrations and the presence of alcoholic hydroxyl groups. The pair bands of 1530−1610 cm^{-1} and 1390−1420 cm^{-1} are assigned to the asymmetric and symmetric stretching vibrations of C-O groups when present as coordinated COO^- moieties.[29] For **5** in solution, the bands from 1540 to 1620 cm^{-1} and 1397 to 1430 cm^{-1} are similar with those of solid state, and no band is seen at 1708 cm^{-1} corresponding to typical free carboxylic group (COOH) of PQC ligand. The additional peaks at 1038 and 954 cm^{-1} can be reasonably attributed to stretching vibration of the S=O groups of free and complexation DMSO molecules, respectively.[30] Thus we can deduce that **5** maintains its structure, where PQC keeps coordination to lanthanide ion in solution.

The thermal gravimetric analysis (TGA) has been performed on **5** as representative to investigate the thermal stabilities with a heating rate of 10 ℃·min^{-1} in the range of 30−1000 ℃ under N_2 atmosphere (Fig. S5†). The TGA curve of **5** indicates two steps of weight losses, where the first step (until 140 ℃) corresponds to removal of two dissociative EtOH molecules with weight loss of 3.9% (calcd 4.4%), and the second step to 220 ℃ corresponds to the further removal of four coordinated solvent molecules with weight loss of 12.6% (calcd 13.3%). Then **5** can keep the thermal stability up to 450 ℃, and after that the framework decomposes gradually.

The crystalline products of **1**−**5** have been characterized by powder X-ray diffraction (PXRD) at room temperature (Fig. S6†). The observed patterns are in good agreement with the results simulated from the single crystal data indicating the purity. The differences in intensity may be due to the preferred orientation of the crystalline powder samples.

Luminescence of Ln_2PQC_6

The luminescent properties of ligand and lanthanide complexes in solid-state were investigated at room temperature (Fig. S7†). For **1**−**3**, broad emission bands at 417, 412 and 417 nm were observed, without characteristic lanthanide emitting. For **4**, except main peak at 423 nm, the spectrum exhibits weak Sm^{3+} emission, centred at 560, 597, 642 and 702 nm, which are assigned to the transitions of $^4G_{5/2} \rightarrow {}^6H_J$ (J = 5/2, 7/2, 9/2, 11/2) respectively. These blue-violet emissions originating from the intraligand π→π* transition of ligand show hypochromatic-shift about 60 nm in comparison to free PQC ligand, due to the rigidity and conjugation changed after formation of the lanthanide coordination complexes. So we can draw a conclusion that triplet state energy level of the ligand mismatches the excited state energy levels of these lanthanide ions.

For **5,** the photoluminescent (PL) spectra in solid state and 95:5 (v/v) EtOH−DMSO solution (1.67×10^{-5} M) are completely different from that of **1**−**4** (Fig. 2). The excitation wavelength (λ_{exc} = 343 nm) was chosen for the most efficient sensitization of the Eu^{3+} luminescence through the antenna effect of PQC. The PL spectrum of solid complex is dominated by characteristic emissions of Eu^{3+} centred at 578, 591, 617, 650 and 696 nm, which originate from corresponding $^5D_0 \rightarrow {}^7F_J$ (J = 0, 1, 2, 3, 4) transitions respectively. PL spectrum in solution is similar, comprising of the Eu^{3+} emissions, except that the enhanced band could be observed for $^5D_0 \rightarrow {}^7F_3$ transition at 650 nm in the case of solution sample and the emission of $^5D_0 \rightarrow {}^7F_4$ is red shifted from 696 nm to 698 nm compared with that of the solid state sample. These tiny differences could be attributed to the solvent effect. In solution, more solvent molecules including EtOH and DMSO may link to metal centre changing the coordination environment slightly to affect the Eu^{3+} emission. The similar phenomenon has been observed normally in previous reports.[31] Absence of broad emission band originating from π → π* transition of PQC, demonstrates the efficient energy transfer from ligand to the emitting levels of europium. The difference in emitting quantum yields (12.50% and 18.71% for **5** in solid and solution, respectively) can be attributed to the molecular aggregation in solid, enhancing the intermolecular interaction, which facilitates the inter- and intra-dinuclear unit Forster energy transfer.[31b] In addition, **5** exhibits characteristic red emission of europium ion under UV 365 nm (insets of Fig. 2) excitation which suggests this complex can be potential red fluorescent material. The CIE chromaticity coordinates of **5** from emission spectra are (0.62, 0.34) in solid, and (0.65, 0.35) in solution, respectively (Fig. S8†).

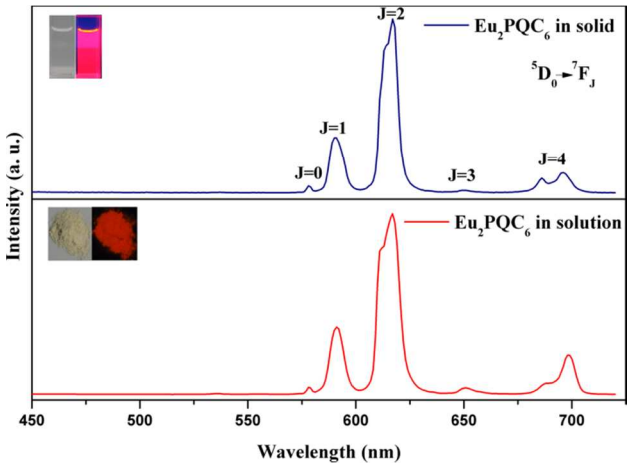

Fig. 2 The room-temperature emission spectra for **5** in solid state and solution under 343 nm excitation. The insets in the upper-left show the color photographs for the brilliant emissions under the UV-light excitation (365 nm).

The sensitivity and selectivity of 5 for anion detection

As described above, complex **5** exhibits a strong red emission. This finding, in addition with the proposed hydrogen-bonding interaction of PQC ligand and the coordination ability of unsaturated europium centre in this complex, offers the inspiration to apply the system as probe for anions. Accordingly, the interactions between a series of anions including F^-, Cl^-, Br^-, I^-, NO_3^-, ClO_4^-, SCN^-, HCO_3^- HSO_4^-, $H_2PO_4^-$, with the **5** have been investigated in solution by using the corresponding three equivalents of Na^+ or TBA salts through UV–vis absorbance and luminescence titrations. The "anion equivalent" denotes the molar ratio of anion titrated into a fixed molar amount of dissolved europium complex. Thus, "1 equiv of anion" means that the anion and receptor are present in equal molar amounts. UV–vis absorbance of **5** and titrations with different anions were measured in EtOH, where no interference from the solvent was present in the region of interest. **5** in EtOH (5×10^{-6} M) gives a transparent solution with two distinguished UV bands at 261 and 327 nm (Fig. 3a), which can be attributed to the $\pi \rightarrow \pi^*$ and $n \rightarrow \pi^*$ transitions of PQC antenna.[20b] Upon sequential addition of 1.88 equal HSO_4^-, a large intensity increase (1.96 and 1.89 folds for two absorption bands, respectively) and a small blue shift to 258 and 324 nm are monitored, respectively, showing that ligand may be partially involved in hydrogen bond formation with the HSO_4^- anions. When $H_2PO_4^-$ replacing HSO_4^-, a little different phenomenon can be observed, where the intensity increase is relatively small (1.45 and 1.32 folds for two absorption bands, respectively) compared with HSO_4^-, and the two transition peaks still remain without shift (Fig. 3b). This observation indicates that there is less ground state interaction between the PQC ligand and $H_2PO_4^-$. Analysis of these intensity changes as a function of added anions is shown as an inset in Fig. 3. The changes in all cases increase significantly before reaching a plateau at about 2.0 equiv of anions. In order to further quantify the reaction ratio between **5** and $H_2PO_4^-$ /HSO_4^- ions, the relevant Job's plot from the UV-vis spectra was constructed by changing the proportion of receptor and anions at a total concentration of 5.0 μm, using a series of **5** solutions with different concentrations as calibration (Fig. S9). For both $H_2PO_4^-$ and HSO_4^-, the maximum point appearing at a molar fraction about 0.33 and is indicative of 1:2 stoichiometry between receptor and analyte. The anion recognition was also monitored by the addition of F^-, Cl^-, Br^-, I^-, NO_3^-, ClO_4^-, SCN^- and HCO_3^- anions (6.0 equiv). In each case, other anions did not cause significant absorption spectral changes and the UV–vis absorption lines remained almost constant, showing that there is insufficient binding to produce changes (Fig. S10†).

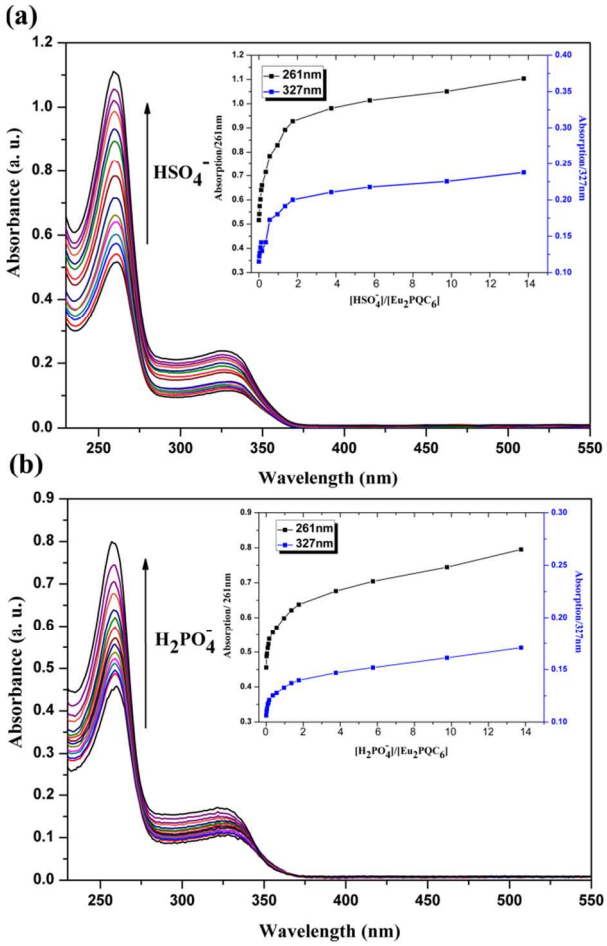

Fig. 3 The changes in the UV–vis absorption spectra of **5** (5×10^{-6} M) in ETOH solution upon addition of (a) HSO_4^- and (b) $H_2PO_4^-$ anion (0–13.8 equiv). Inset: the plot of intensities of the sensing ensemble at 261nm and 327 nm, respectively *versus* anion concentration.

In parallel to the absorption spectra, the obtained emission spectra and bar diagrams based on the relative emission intensities indicate that the quenching of the emission by HSO_4^- and $H_2PO_4^-$ ions is remarkable (Fig. 4). Upon titration, the intensity of maximum peak at 617 nm decreases significantly, resulting in 98% and 91% quenching after the addition of 3.0 equiv of HSO_4^- and $H_2PO_4^-$ ions respectively. While the addition of F^-, Cl^-, Br^-, I^-, NO_3^-, ClO_4^-, SCN^- anions results in a variation range of the relative emission intensity from 0.87 to 1.13 with respect to the parent **5**. These anions give no distinct response to the PL spectra in solution, except HCO_3^-, inducing 37% luminescence quenching. However, such degree of quenching is much weak compared with that by HSO_4^- and $H_2PO_4^-$. In this work, we further investigated the selectivity of the **5** as sensor for HSO_4^- and $H_2PO_4^-$ in the presence of other anions. For this

purpose, **5** was treated with 3.0 equiv of HSO_4^- or $H_2PO_4^-$ in the presence of competing ions (6.0 equiv). The luminescence quenching degree (I/I_0) of this sensor is always > 85%, which does not appear to have any obvious changes compared with that in the absence of other anions (Fig. S11†). These behaviors clearly demonstrate that **5** is efficient capable of recognizing HSO_4^- or $H_2PO_4^-$ in highly competitive media.

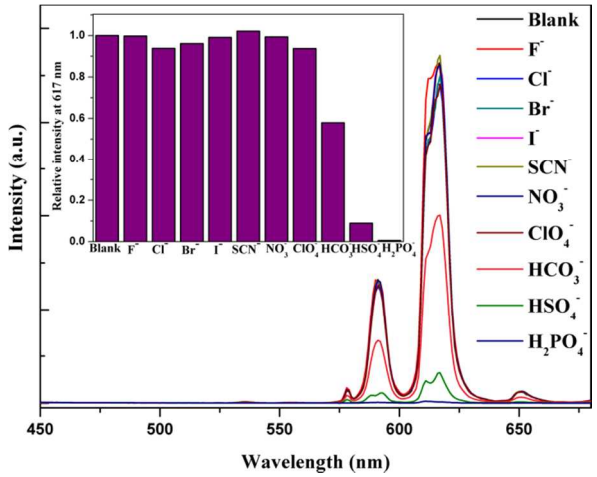

Fig. 4 Luminescence quenching response of **5** (1.67×10^{-5} M) against various anions (3.0 equiv were added): Emission spectra (λ_{exc} = 343 nm) of **5** and bar diagram (inset) showing relative intensities of the emission peak at 617 nm.

The significant emission changes for HSO_4^- and $H_2PO_4^-$ encourage us to choose these two anions for further studies. A systematic titration has been performed, incrementing the concentration of HSO_4^- and $H_2PO_4^-$ from 0.01 to 22 equiv. Firstly, as shown in Fig. 5a, excited by 343 nm, upon tradition of HSO_4^-, it is observed that the intensity of the maximum band at 617 nm decreased significantly and other emission bands ($^5D_0 \rightarrow {}^7F_0$, $^7F_1$, $^7F_3$, $^7F_4$) are affected similarly, leading to a 90% quenching after the addition of 2.88 equiv of anions. Notably, the fluorescence intensity changed almost linearly with the concentration of HSO_4^- in the range of 0–33.4 μM. A major advantage for this europium probe is the incorporation of ratiometric imaging, where the magnetic dipole induced J=1 transition is relative insensitive to changes in coordination, whereas J=2 transition is hypersensitive. Interestingly, over the course of HSO_4^- addition, the emission ratio of I_{617nm}/I_{591nm} maintained about 2.8 without large change, which excludes the possibility of perturbation in the coordination environment around Eu^{3+} centre. Analysis of these changes as a function of added HSO_4^- is shown as an inset in Fig. 5a. The intensity of emitting at 617 nm decreases significantly before reaching a plateau at about 2.0 equiv of HSO_4^-, demonstrating again that **5** interacts with added ions in a 1:2 stoichiometry. The absence of any change (apart from a loss in intensity) in the excitation spectra corroborates the corresponding mirror image of this quenching (Fig. S12†). Simultaneously, the anion titration experiments have been monitored at an excitation wavelength of 395 nm (Fig. 5b), where Eu^{3+} is excited directly ($^7F_0 \rightarrow {}^5L_6$) and ligand has no absorption. As expected, there is no change in the luminescence intensity outside of what would be expected for dilution over the course of titration (reduced by 1.5% and 9.4% for 591 and 617nm, respectively), when the Eu^{3+} ion is directly excited (inset in Fig. 5b), indicating that the lanthanide ion does not participate in anion binding.

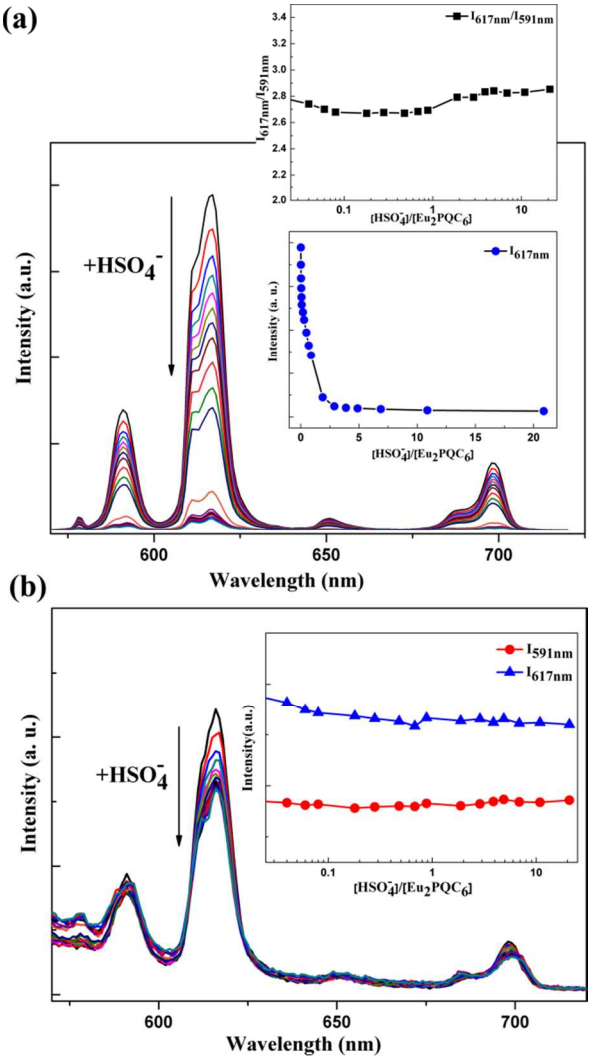

Fig. 5 Luminescence of **5** upon titration with HSO_4^- (0−22 equiv) in 95:5 (v/v) EtOH−DMSO solution (1.67×10^{-5} M): (a) Excitation at λ_{exc} = 343 nm. Inset: changes in the ratio of I_{617nm}/I_{591nm} and I_{617nm} of Eu^{3+} emission *versus* equiv of HSO_4^- added; (b) Direct excitation at λ_{exc} = 395 nm. Inset: changes in I_{591nm} and I_{617nm} of Eu^{3+} emission *versus* equiv of HSO_4^- added.

In the case of $H_2PO_4^-$ ion, the situation was totally different in detail, although the quenching was similar in outward manifestation. As shown in Fig. 6a, upon addition of $H_2PO_4^-$, the intensity of maximum peak at 617 nm decreases dramatically, resulting in a 98% quenching after titration of 2.88 equiv of anion (λ_{exc} = 343 nm). Similarly, the fluorescence intensity shows linear change with the concentration of $H_2PO_4^-$ in the range of 0–33.4 μM. Moreover, $H_2PO_4^-$ shows distinct behaviour with peak splitting at J=2 transition (new band at 611 nm) along with a remarkable decrease in the emission ratio of I_{617nm}/I_{591nm} from 2.8 to 1.3, which reflects the variation in the coordination environment of Eu^{3+}. Analysis of these changes as a function of added $H_2PO_4^-$ is shown as an inset in Fig. 6a. The changes in all cases decrease significantly before reaching a plateau at about 2.0 equiv of $H_2PO_4^-$, demonstrating that **5** interacts with $H_2PO_4^-$ in a 1:2 stoichiometry. As our prediction, for $H_2PO_4^-$, the change of

the emission intensity at 617 nm was obvious (reduced by 75%), when Eu^{3+} was directly excited at 395 nm during titrations (Fig. 6b). This observation indicates that the original coordination environment around Eu^{3+} has been interrupted, which is consisted with above fluorescence results. Meanwhile the absence of any changes (apart from a loss in intensity) in the excitation spectrum monitored at 617 nm also corroborates the fact that the quenching of Eu^{3+}-based emission is the pure result of coordination solvents displacement during the titration (Fig. S12†).

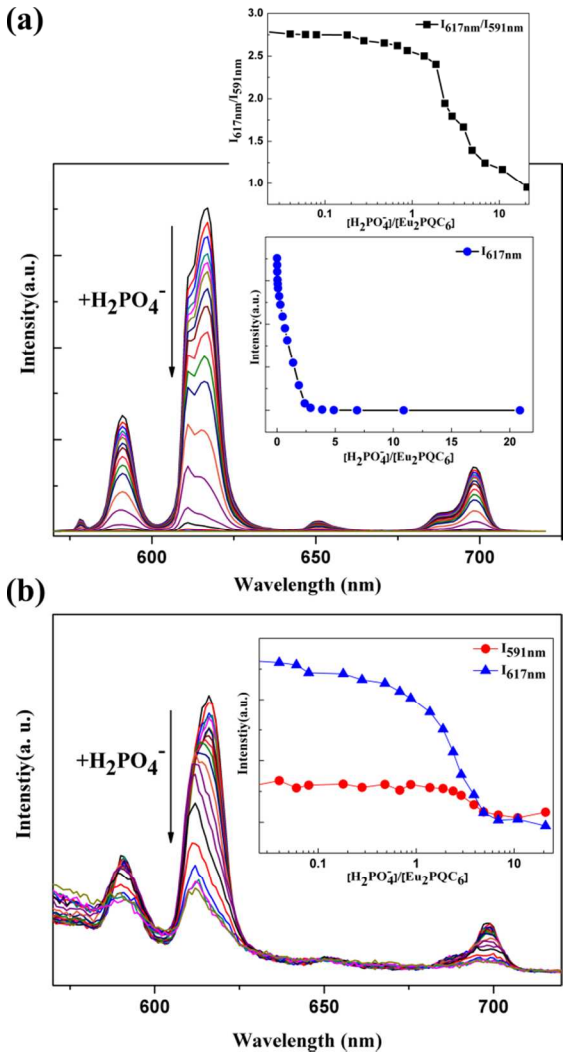

Fig. 6 Luminescence of **5** upon titration with $H_2PO_4^-$ (0−22 equiv) in 95:5 (v/v) EtOH−DMSO solution (1.67×10^{-5} M): (a) Excitation at λ_{exc} = 343 nm. Inset: changes in the ratio of I_{617nm}/I_{591nm} and I_{617nm} of Eu^{3+} emission *versus* equiv of $H_2PO_4^-$ added; (b) Direct excitation at λ_{exc} = 395 nm. Inset: changes in I_{591nm} and I_{617nm} of Eu^{3+} emission *versus* equiv of $H_2PO_4^-$ added.

Based on the titration, the response parameter **α**, which is defined as the ratio of the non-interaction **5** concentration to the initial concentration, is plotted as a function of HSO_4^- and $H_2PO_4^-$ concentration (Fig. S13†). The corresponding association constants (Table 1) are determined as $\log K_a$ = 3.68 and 3.81, by using double logarithm regression equation: $\log[(I_0 - I)/(I - I_{min})] = 1/\Delta I = \log K_a + n\log([anion])$,[32] where I_0, I, and I_{min} are the emission intensities of **5** in the absence of HSO_4^- or $H_2PO_4^-$, at varying amounts of HSO_4^- or $H_2PO_4^-$, at a concentration of the complete interaction, respectively, and n is the number of each anion bound to **5**. The linear fit with n = 0.63 and 0.68, indicates a 1: 2 ratio for the interaction between HSO_4^-, $H_2PO_4^-$ and the europium complex (Fig. S14†). The LOD for this recognition process is determined as 1.50 and 0.83×10^{-8} M for HSO_4^- and $H_2PO_4^-$, respectively (using 2.7 mL samples) by monitoring the sensitive changes in the Eu^{3+} emission (Fig. S15†), which has achieved the lowest level compared with the data reported.[10,11] The LOD can be orders of magnitude lower than the probes based on organic ligands (from μM to nM), so this europium based sensor has potential application in trace analysis. Furthermore, the emission is found to be responds quickly to the anions, owing to the fast interaction process. Repeated measurements show that the emission intensity immediately decreases nearly down to minimum after the addition of anions, providing a ''zero-wait'' detecting method (Fig. S16†).

Table 1 Photophysical properties of sensor complex for HSO_4^- /$H_2PO_4^-$

Anion	Quenching	Association constant (K_a)	Limit of detection (LODs)
HSO_4^-	91%	3.68	1.53×10^{-8} M
$H_2PO_4^-$	98%	3.81	0.83×10^{-8} M

Mechanism of anion recognition

According to our predesign and the PL results, the change of luminescent signal caused by HSO_4^- can be assumed to the anion hydrogen-binding with PQC, leading to more electron-rich antennae, which could alter the efficiency of energy transfer to the Eu^{3+} centre. The limit of 1:2 stoichiometry can be reasonably attributed to the electrostatic repulsion from negative charge aggregation, despite of more potential hydrogen-bonding sites from six PQC ligands in one probe molecule. For the process of $H_2PO_4^-$ addition, the quenching mechanism here involves $H_2PO_4^-$-induced displacement of EtOH from the first coordination sphere of Eu^{3+} centre caused by complexation. Coordination of phosphate may happen through a monodentate binding mode or potentially as a bidentate ligand.[33] This behaviour indicates less efficient energy transfer processes, but substantial decrease of the detrimental nonradiative deactivation pathways in the ternary species. The energy migration process from ligand to europium ion is terminated by coordination of $H_2PO_4^-$ anions, through breaking the previous intersystem crossing process of ligand and suppressing the population of triplet state. Therefore, the singlet emission from PQC may take over during the $H_2PO_4^-$ titration. According to analysis of PL, the significant augmentation by 65% of emission intensity at 387 nm from ligand has actually occurred, while the responding intensity almost remained the same during HSO_4^- titration (Fig. S17†). This obvious distinction offers another way to identify HSO_4^- from $H_2PO_4^-$.

In order to corroborate this result, X-ray photoelectron spectroscopy (XPS) experiments were then carried out on pure tetrabutylammonium (TBA) salt $[TBA]H_2PO_4$, **5**, and the binary complexation sample **5**-H_2PO_4 (**5** disperses in EtOH with two equiv $[TBA]H_2PO_4$ and undergoes centrifugation, washing and drying). The reference line of C 1s specified for C-C bond is used as calibration for the present spectra. As shown in Fig. S18, the observed asymmetry in the P 2p spectra which leaded to the deconvolution into two peaks could arise from the spin–orbit splitting of the P 2p core level resulting in the distinguishable P $2p_{3/2}$ and P $2p_{1/2}$ core levels with the lower binding energy peak

corresponding to P $2p_{3/2}$. It is apparent that the peak of P 2p moved to a higher value after complexation, where P $2p_{3/2}$ shifted from 132.03 to 133.43 eV and P $2p_{1/2}$ shifted from 132.40 to 134.43 eV, respectively. It is worth mentioning that the peak appearing at 135.93 eV during the P element detection results from Eu 4d level. The binding energies of Eu 3d for **5** was observed at 1134.78 eV, which shifted to higher binding energies by 0.6 eV to 1135.38 eV for **5**-$H_2PO_4^-$ after $H_2PO_4^-$ addition. These shifts about binding energies of P 2p and Eu 3d indicate that the chemical environments of Eu and P atoms have been changed after the interaction, which can be attributed to the formation of Eu-O-P bonds.[34]

To better understand the interaction mode between **5** and anions, the ^{1}H NMR titrations of HSO_4^- and $H_2PO_4^-$ with **5** were used for more precisely study in DMSO-d_6. It is evident from Fig. 7a, addition of HSO_4^- to **5** (8.0 mM) results in a downfield shift and broadening of resonances, again indicating that the aromatic and quinoline ring played an important role in binding HSO_4^-. The following disappearance of H_a and H_b peaks at δ 7.12 and 7.25, indicates the deprotonation of C atoms during complexation. Enduring 2.0 equiv of HSO_4^-, the H_c signal appears at δ 8.63, indicating that protonation of the N atom in quinoline group has occurred. This observation is in good agreement with the formation of strong hydrogen-bonding interactions between HSO_4^- and PQC ligand.[19a,31b] The interaction mode has been shown in Fig.7a, where just PQC and HSO_4^- are considered for simplification. During the titration of $H_2PO_4^-$, the C–H signals shift downfield by 0.03–0.14 ppm at 2.0 equiv of anion (Fig. 7b). The slight signal change indicates the surrounding of PQC is not interrupted, which confirms our hypothesis that $H_2PO_4^-$ prefers coordination to metal centre directly rather than interaction with PQC ligand.[19b] Moreover, for these two anions, excess additions up to 3.0 equiv of anions, do not affect the spectra virtually, indicating that **5** bonded to HSO_4^- and $H_2PO_4^-$ ions with 1:2 stoichiometry. It is worth mentioning that the ^{1}H NMR spectra about binary substrates **5**-$H_2PO_4^-$ and **5**-HSO_4^- are similar to that of parent sample **5** with some degree of peak translation, while the characteristic peaks for free PQC does not appear (Fig. S19). Therefore the possibility of decomposition could be excluded, demonstrating the stability of probe molecule during the sensing experiments.

A comprehensive understanding of the nature of the different interaction modes between HSO_4^-, $H_2PO_4^-$ and sensor, which is crucial to design novel materials and improve their sensitivity and selectivity for further application, is still lacking. Therefore, to shed light on the origin of different recognition mechanisms, an in-depth investigation from the perspective of theory is necessary. Based on above discussion, we calculated the interaction energies between the selected anions and **5** by the DFT method with the hybrid Becke three-parameter Lee-Yang-Parr functional at B3LYP/6-31++G* and 6-31G** levels, respectively. (Detail of the calculation has been shown in experiment section.) For simplification, the PQC-HSO_4^-/$H_2PO_4^-$ modes for hydrogen-bonding interaction and Eu-HSO_4^-/$H_2PO_4^-$ modes for coordination-bonding interaction have been considered respectively (Fig. S20†). It has been found, the hydrogen bonding interaction energy about HSO_4^- with PQC ligand is larger than that of $H_2PO_4^-$, while the interaction energy about $H_2PO_4^-$ with Eu^{3+} centre through coordination is large compared with that of HSO_4^- in both monodentate and bidentate modes (Table 2). The contrast interaction ability may originate from different stereochemical effects and electronegativities.[35] The exhaustive data including hydrogen bond length and interaction energies have been shown in Table S3-S6†. It means that in presence of different anions, **5** prefers the most stable state through different interaction modes. The calculated result can explain the experiments and supports our conclusion well, based on which, the tentative structures for the interaction of HSO_4^- and $H_2PO_4^-$ with **5** can be proposed (Fig. 8). Additionally, the red fluorescence of **5** disappeared after the addition of anions, and this was easily detected by the naked eye.

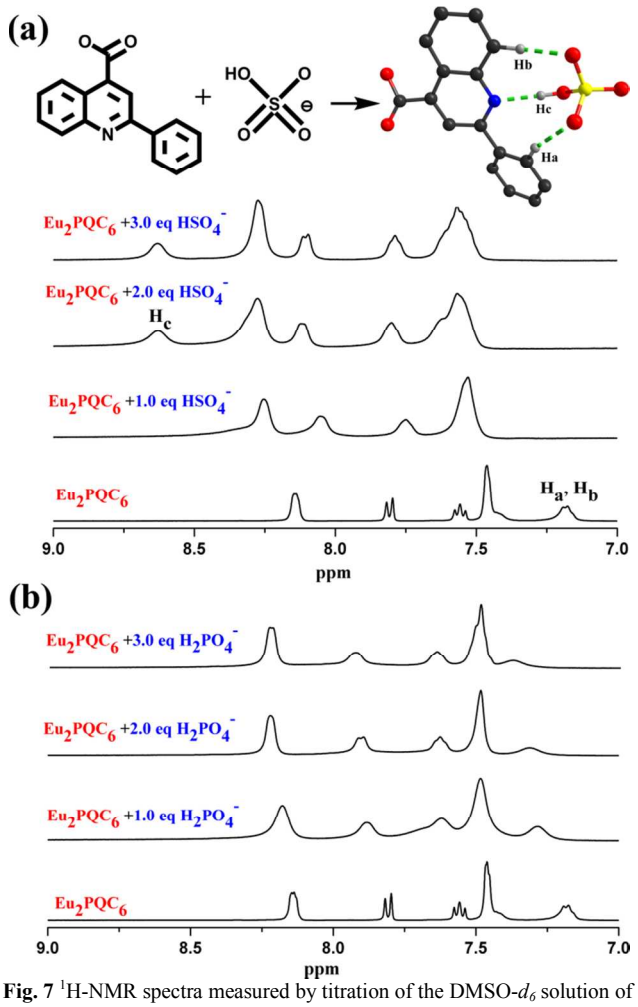

Fig. 7 ^{1}H-NMR spectra measured by titration of the DMSO-d_6 solution of 5 (8.0 mM) with 1.0–3.0 equiv of (a) [TBA]HSO_4 and (b) [TBA]H_2PO_4.

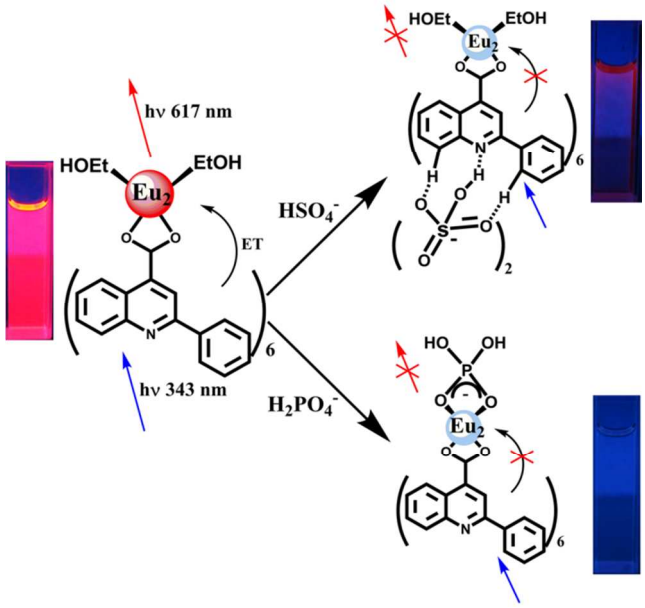

Fig. 8 Proposed binding modes of HSO_4^- and $H_2PO_4^-$ with the **5** sensor. In the absence of the anion, excitation of PQC followed by energy transfer to the lanthanide enables bright red luminescence centered at 617 nm. Interaction of anions favors quenching of the antenna and, consequentially, also that of the Eu^{3+} luminescence.

Table 2 The calculated interaction energy about $HSO_4^-/H_2PO_4^-$ with PQC and Eu^{3+} in different modes by DFT method.

Anion	Hydrogen bonding interaction energy (kcal/mol)	Coordination bonding interaction energy in monodentate mode (kcal/mol)	Coordination bonding interaction energy in bidentate mode (kcal/mol)
HSO_4^-	-3.35569	-59.16024	-70.58065
$H_2PO_4^-$	-3.25048	-63.62655	-74.78070

Responds to anionic bio-phosphates

To meet the application requirements for biological and environmental detection, the fluorescence of **5** was tested in mixed aqueous solutions (H_2O-DMSO solution with different volume ratios). The results show that the major emitting peak at 617 nm can maintain 41% intensity with 10% water, which can be attributed to the coordination of H_2O molecules to Eu^{3+} centre by substitution of terminal ETOH (Fig. S21†). The O–H oscillators trigger non-radiative scattering processes.[36] Furthermore, the lifetimes of emission at 617 nm, in 10:90 (v/v) H_2O-DMSO and D_2O-DMSO solution, have been recorded as $\tau_{H2O} = 0.57$ ms and $\tau_{D2O} = 1.15$ ms, respectively. The number of coordinated water molecules (q) to each Eu^{3+} centre for **5** in aqueous solution can be calculated from the equation $q = A((\tau_{H2O}^{-1} - \tau_{D2O}^{-1}) - k_{corr})$, with $A = 1.2$, $k_{corr} = 0.25$ ms^{-1},[37] from which $q = 0.77$ has been determined (Fig. S22†).

Because **5** gives a sensitive and selective emission response to phosphate ions, this work has been extended to the sensing of nucleosides AMP, ADP and ATP in mixed aqueous solution. As shown in Fig. 9, these bio-phosphates show quenching with different specificities in detectable range. The emission intensity at 617 nm reduces to 18.5, 0.5 and 55.7%, after the addition of 5.0 equiv of ATP, ADP and AMP, respectively. Thus, the intensity difference ranges between about 18–55% as a result of the interaction with the nucleoside phosphates. Complex **5** has distinguishable responses in presence of different nucleoside phosphates, therefore it acts as a "special" luminescent sensor for the determination of three phosphates. On the basis of this outcome, a systematic fluorescence titration has been carried out and the respective binding constant for ATP, ADP and AMP is $\log K_a = 3.42$, 5.99 and 2.64, respectively, as derived from the linear fits (Fig.10 and Fig. S23†). This data clearly indicates that the ADP anion binds most strongly. Although the coordination of $H_2PO_4^-$ and ADP resulted in similar photophysical perturbations, it is surmised that the coordination behaviour of these two species is not the same. The coordination of ADP can occur through the formation of six membered chelate rings, through the oxygen atoms of the phosphorylated chain.[38] This rare selectivity for ADP can be attributed to the tentative reasons as follow: (1) The tripositive Eu^{3+} metal centre preferably interacts with anion possessing higher negative charge, so the quenching caused by ATP and ADP is much stronger than that of AMP; (2) Taking the stereo-hindrance effect into account, the length of the diphosphate arm chain of ADP may fit well for molecular model of **5** to realize the coordinated interactions, or the potential $\pi\cdots\pi$ stacking interactions between the purine and aromatic ring, and the remaining hydroxyl function implication in an intramolecular hydrogen bond with the nitrogen atom of the ligand.[39] Thereby, this complexation prevents energy transfer from the antenna to the lanthanide and consequently quenching Eu^{3+} luminescence.

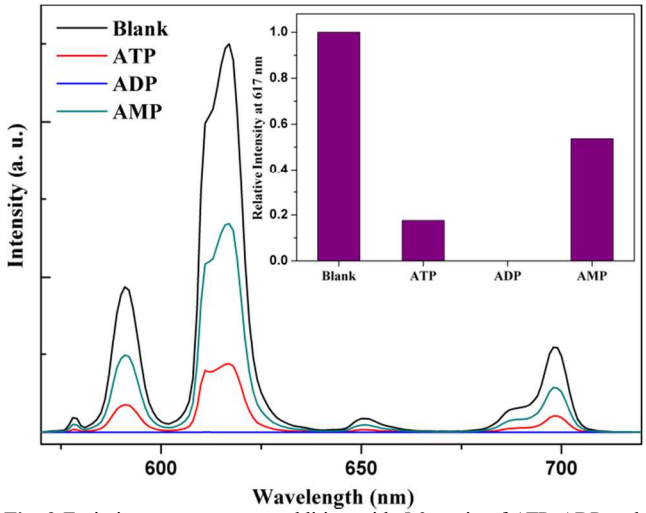

Fig. 9 Emission response upon addition with 5.0 equiv of ATP, ADP and AMP nucleoside phosphates in 10:90 (v/v) H_2O-DMSO solution to **5** (1.67×10^{-5} M). Bar diagram (inset) shows relative intensities of the emission peak at 617 nm.

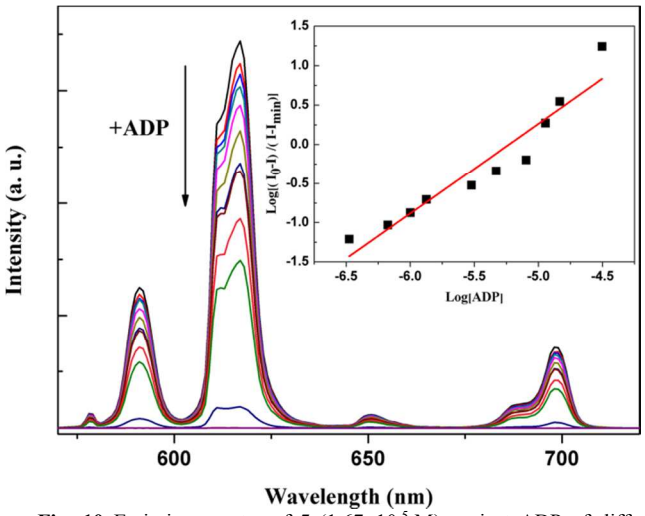

Fig. 10 Emission spectra of **5** (1.67×10^{-5} M) against ADP of different concentrations in 10:90 (v/v) H_2O-DMSO solution. The inset shows the linear fit related to the binding constant determination.

Conclusion

Herein, we have discussed the synthesis and the characterization of a series of PQC-based lanthanide complexes $\mathbf{Ln_2PQC_6}$. The crystal structures obtained for the dinuclear complexes give some understanding of the geometry, where lanthanide centre cooperates with two EtOH molecules as part of coordination sphere and the quinolyl N atoms of PQC are uncoordinated. All lanthanide complexes mainly show ligand-centred emissions, except **5** with a strong characteristic red emission. This fluorescent system, possessing both potential hydrogen-bond-accepting sites from PQC ligand and unsaturated europium centre with replaceable coordinated solvent molecules, is designed to become a unique anion probe through multiple binding interactions. Because of the peculiar O–H---N hydrogen-bond interaction and direct coordination mode within a single structure, this complex is expected to recognize hydrogenous anions with high selectivity excluding interference of competitive anions. According to relevant PL results, **5** displays a high affinity towards HSO_4^- and $H_2PO_4^-$, showing quenching of luminescence signal with very low detection limits (15.3 and 8.3 nM respectively in the linear range of 0–33.4 μM). As expected, the combined studies of experimental and theoretical characterizations including meticulous UV-Vis, NMR spectroscopy titration experiments, XPS analysis, stability constant estimations, and anion-responsive luminescence measurements indicate that the similar quenching effects of two anions derive from above different mechanisms actually. In general, we have demonstrated the use of novel probe to bind anions via various binding interactions, consisting of both hydrogen bonding for HSO_4^- and metal coordination for $H_2PO_4^-$ respectively. Specially, through quantum chemical DFT calculation, we obtain in-depth understanding of complexation process based on interaction energy, which explains the experiment and support our hypothesis well. Moreover, on the basis of this finding, work has been extended to detection of adenosine phosphates and a high luminescent specificity for ADP over ATP and AMP could be achieved. A reasonable binding model can be suggested and the regarding the high association constant for ADP, may be due to some effective total of multiple bindings. This luminescent sensitive complex can be applied in trace analysis and the "multiple-interaction" mode can serve as a platform to design anion probe with high sensitivity and selectivity. Pursuing further studies on recognition mechanism of adenosine phosphates and design of lanthanide complexes for detection in aqueous solution are underway. We believe that the present system will provide useful information to the range of luminescent probe that can operate at molecular level. These results are promising in regard to the application of these lanthanide complexes to sensing anionic species in biological and environmental science.

Acknowledgements

The authors are grateful to National Nature Science Foundation of China (Grants 91022035), Natural Science Funds of Fujian Province (Grant 2014H0055) and CAS hundred talents program for financial support of this work.

Notes and references

[a] *Key Laboratory of Optoelectronic Materials Chemistry and Physics, Fujian Institute of Research on the Structure of Matter, Chinese Academy of Sciences, Fuzhou, 350002,China. Fax:+86-591-63173227;Tel: +86-591-63173227;E-mail: yfzhou@fjirsm.ac.cn*
[b] *University of the Chinese Academy of Sciences, Beijing, 100049, China*

† Electronic Supplementary Information (ESI) available: Tables for crystallographic data and DFT calculation, additional structal, photoluminescent spectra and lifetimes analysis and molecular diagrams. For ESI and crystallographic data in CIF or other electronic format see DOI: 10.1039/b000000x/

1 (a) O. Augusto, M. G. Bonini, A. M. Amanso, E. Linares, C. Santos and S. L. De Menezes, *Free Radic. Biol. Med.*, 2002, **32**, 841; (b) P. Pacher, J. S. Beckman and L. Liaudet, *Physiol. R*ev., 2007, **87**, 315; (c) S. Kubik, *Chem. Soc. Rev.*, 2010, **39**, 3648; (d) A. Bianchi, K. B. James and E. G. España, *Supramolecular Chemistry of Anions*, Wiley-VCH: New York, 1997; (e) K. L. Kirk, *Biochemistry of the halogens and inorganic halides*, Plenum Press, New York, 1991.

2 (a) J. O. Lundberg, E. Weitzberg and M. T. Gladwin, *Nat. Rev. Drug Discov.*, 2008, **7**, 156; (b) P. A. Gale, *Acc. Chem. Res.*, 2011, **44**, 216; (c) F. Okamoto, H. Kajiya, K. Toh, S. Uchida, M. Yoshikawa, S. Sasaki, M. A. Kido, T. Tanaka and K. Olabe, *Am. J. Physiol. Cell Physiol.*, 2008, **294**, C693.

3 (a) K. Li, T. He, C. Li, X. W. Feng and X. Q. Yu, *Green Chem.*, 2009, **11**, 777; (b) A. Robertson and S. Shinkai, *Coord. Chem. Rev.*, 2000, **205**, 157.

4 (a) F. P. Schmidtchen, M. Berger, *Chem. Rev.*, 1997, **97**, 1609; (b) K. J. Chang, B. N. Kang, M. H. Lee and K. S. Jeong, *J. Am. Chem. Soc.*, 2005, **127**, 12214; (c) T. Yamaguchi, S. Tashiro, M. Tominaga, M. Kawano, T. Ozeki and M. Fujita, *Chem. Asian J.*, 2007, **2**, 468; (d) C. Suksai and T. Tuntulani, *Chem. Soc. Rev.*, 2003, **32**, 192.

5 (a) A. Mallick, T. Katayama, Y. Ishibasi , M. Yasudab and H. Miyasaka, *Analyst*, 2011, **136**, 275; (b) C. F. Wan, S. T. Yang, H. Y. Lin, Y. J. Chang and A. T. Wu, *Luminescence*, 2014, **29**, 500; (c) H. J. Kim, S. Bhuniya, R. K. Mahajan, R. Puri, H. G. Liu, K. C. Ko, J. Y. Lee and J. S. Kim, *Chem Commun.*, 2009, 7128; (b) S. T. Yang, D. J. Liao, S. J. Chen, C. H. Hu and A. T. Wu, *Analyst*, 2012, **137**, 1553.

6 (a) G. A. Block and F. K. Port, *Am. J. Kidney Dis.*, 2000, **35**, 1226; (b) W. Saenger, *Principles of Nucleic Acid Structure*, Springer, Heidelberg, 1998; (c) D. A. Johnson, P. Akamine, E. Radzio-Andzelm, M. Madhusudan and S. S. Taylor, *Chem. Rev.*, 2001, **101**, 2243; (d) A. V. Gourine, E. Llaudet, N. Dale and M. Spyer, *Nature*, 2005, **436**, 108.

7 K. T. Bush, S. H. Keller and S. K. Nigam, *J. Clin. Invest.*, 2000, **106**, 621.

8 (a) N. D. Toussaint, E. Pedagogos, S. J. Tan, S. V. Badve, C. M. Hawley, V. Perkovic and G. J. Elder, *Nephrology*, 2012, **17**, 433; (b) C. Zoccali, P. Ruggenenti, A. Perna, D. Leonardis, R. Tripepi, G. Tripepi, F. Mallamaci and G. Remuzzi, *J. Am. Soc. Nephrol.*, 2011, **22**, 1923.

9 (a) C. Suksai and T. Untulani, *Chem. Soc. Rev.*, 2003, **32**, 192; (b) V. Amendola, D. E. Gomez, L. Fabbrizzi and M. Licchelli, *Acc. Chem. Res.*, 2006, **39**, 343; (c)L. J. Charbonniere, R. Schurhammer, S. Mameri, G. Wipff and R. F. Ziessel, *Inorg. Chem.*, 2005, **44**, 7151;(d) X. M. Liu, Q. Zhao, W. C. Song and X. H. Bu, *Chem. Eur. J.*, 2012, **18**, 2806; (e) T. Gunnlaugsson, M. Glynn, G. M. Tocci, P. E. Kruger and F. M. Pfeffer, *Coord. Chem. Rev.*, 2006, **250**, 3094; (f) S. J. Butler and D. Parker, *Chem. Soc. Rev.*, 2013, **42**, 1652; (g) Y. Kataoka, D. Paul, H. Miyake, S. Shinoda and H. Tsukube, *Dalton Trans.*, 2007, 2784.

10 (a) M. Alfonso, A. Tárraga and P. Molina, *Org. Lett.*, 2011, **13**, 6432; (b) P. Li P, Y. M. Zhang, Q. Lin, J. Q. Li and T. B. Wei, *Spectroc. Acta Pt. A*, 2012, **90**, 152; (c) L. Wang, L. Yang and D. Cao, *J. Fluoresc.*, 2014, **24**, 1347; (d) C. L. Tan and Q. M. Wang, *Inorg. Chem.*, 2011, **50**, 2953; (e) P. Kaur, H. Kaur, K. Singh, *Analyst*, 2013, **138**, 425.

11 (a) B. H. M. Snellink-Ruël, M. M. G. Antonisse, J. F. J. Engbersen, P. Timmerman and D. N. Reinhoudt, *Eur. J. Org. Chem.*, 2000, 165; (b) J. L. J. Blanco, P. Bootello, J. M. Benito, C. O. Mellet and J. M. G. Fernández, *J. Org. Chem.*, 2006, **71**, 5136; (c) H. K. Cho, D. H. Lee, J. Hong, *Chem. Commun.*, 2005, 1690; (d) O. Reynes,; J. C. Moutet, J. Pecaut, G. Royal and E. Saint-Aman, *New J. Chem.*, 2002, **26**, 9; (e) Z. J. Chen, L. M. Wang, G. Zou, X. M. Cao, Y. Wu and P. J. Hu, *Spectroc. Acta Pt. A*, 2013, **114**, 323.

12 (a) P. Zhao, J. B. Jiang, B. Leng and H. Tian, *Macromol. Rapid Commun.*, 2009, **30**, 1715; (b) S. O. Kang, R. A. Begum, K. Bowman-James, *Angew. Chem., Int. Ed.*, 2006, **45**, 788; (c) Y. Qu, J. L. Hua, Y. H. Jiang and H. Tian, *J. Polym. Sci., Part A: Polym. Chem.*, 2009, **47**, 1544.

13 (a) M. A. Palacios, R. Nishiyabu, M. Marquez and P. Anzenbacher, *J. Am. Chem. Soc.*, 2007, **129**, 7538; (b) F. P. Schmidtchen, *Org. Lett.*, 2002, **4**, 431.

14 (a) X. M. He, F. Herranz, E. C. C. Cheng, R. Vilar and V. W. W. Yam, *Chem. Eur. J.*, 2010, **16**, 9123; (b) M. Boiocchi, L. Del Boca, D. E. Gomez, L. Fabbrizzi, M. Licchelli and E. Monzani, *J. Am. Chem. Soc.*, 2004, **126**, 16507; (c) G. X. Xu and M. A. Tarr, *Chem. Commun.*, 2004, 1340.

15 (a) K. Dhanunjayarao, V. Mukundam and K. Venkatasubbaiah, *J. Mater. Chem. C*, 2014, **2**, 8599; (b) D. A. Jose, D. K. Kumar and B. Ganguly, A. Das, *Org. Lett*., 2004, **6**, 3445; (c) A. F. Li, J. H. Wang, F. Wang and Y. B. Jiang, *Chem. Soc. Rev.*, 2010, **39**, 3729.

16 (a) J. M. Hu, C. H. Li, Y. Cui and S. Y. Liu, *Macromol. Rapid Commun.*, 2011, **32**, 610; (b) N. Kumari, S. Jha and S. Bhattacharya, *J. Org. Chem.*, 2011, **76**, 8215; (c) C. Bhaumik, D. Maity, S. Das and S. Baitalik, *RSC Adv.*, 2012, **2**, 2581; (d) R. M. F. Batista, E. Oliveira, S. P. G. Costa, C. Lodeiro and M. M. M. Raposo, *Org. Lett.*, 2007, **9**, 3201; (e) C. Bhaumik, S. Das, D. Maity and S. Baitalik, *Dalton Trans.*, 2011, **40**, 11795.

17 (a) H. Xia, J. Li, G. Zou, Q. Zhang and C. Jia, *J. Mater. Chem. A*, 2013, **1**, 10713; (a) A. J. Harte, P. Jensen, S. E. Plush, P. E. Kruger and T. Gunnlaugsson, *Inorg. Chem.*, 2006, **45,** 9465; (b) Q. M. Wang and H. Tamiaki, *J. Photochem. Photobiol. A*, 2009, **206**, 124; (c) S. Saha, A. Ghosh, P. Mahato, S. Mishra, S. K. Mishra, E. Suresh, S. Das and A. Das, *Org. Lett.*, 2010, **12**, 15; (d) C. Kihang and A. D. Hamilton, *Angew. Chem., Int. Ed.*, 2001, **40**, 3912; (e) J. Y. Jo and D. W. Lee, *J. Am. Chem. Soc.*, 2009, **131**, 16283; (f) Z. M. Hudson, X. Y. Liu and S. N. Wang, *Org. Lett.*, 2011, **13**, 2; (g) H. B. Yu, Q. Zhao, Z. X. Jiang, J. G. Qin and Z. Li, *Sens. Actuators, B*, 2010, **148**, 110; (h) N. Kumari, S. Jha and S. Bhattacharya, *J. Org. Chem.*, 2011, **76**, 8215; (i) S. Y. Chung, S. W. Nam, J. Lim, S. Park and J. Yoon, *Chem. Commun*., 2009, 2866; (j) X. M. Liu, Y. P. Li, W. C. Song, Q. Zhao and X. H. Bu, *Talanta*, 2012, **97**, 111.

18 (a) Y. H. Han, C. B. Tian, Q. H. Lia and S.W. Du, *J. Mater. Chem. C,* 2014, **2**, 8065; (b) Y. Li, J. Li, L. Wang, B. Zhou, Q. Chen and X. Bu, X. *J. Mater. Chem. A*. 2013, **1**, 495; (c) Y. M. Zhu, C. H. Zeng, T.S. Chu, H. M. Wang, Y. Y. Yang, Y. X. Tong, C.Y. Su and W. T. Wong, *J. Mater. Chem. A*, 2013, **1**, 11312; (d) E. G. Moore, A. P. S. Samuel and K. N. Raymond, *Acc. Chem. Res.*, 2009, **42**, 542; (e) R. A. Poole, F. Kielar, S. L. Richardson, P. A. Stenson and D. Parker, *Chem. Commun.*, 2006, 4084; (f) D. Parker and J. Yu, *Chem. Commun*., 2005, 3141; (g) R. Pal and D. Parker, *Org. Biomol. Chem.*, 2008, **6**, 1020; (h) Z. Zhou, Q. M. Wang, M. HuoS and Y. Q. Yang, *Photochem. Photobiol. Sci.*, 2012, **11**, 738; (i) C. M. G. Santos and T. Gunnlaugsson, *Supramol. Chem.*, 2009, **21**, 173; (j) C. M. G. Santos, P. B. Fernandez, S. E. Plush, J. P. Leonard and T. Gunnlaugsson, *Chem. Commun*., 2007, 3389; (h) C. B. He, K .D. Lu and W. B. Lin, *J. Am.Chem. Soc.*, 2014, **136**, 12253.

19 (a) C. G. Gulgas and T. M. Reineke, *Inorg. Chem.*, 2008, **47**, 1548; (b) Q. Wang, C. Tan, H. Tamiaki and H. Chen, *Photochem. Photobiol. Sci.*, 2010, **9**, 791; (c) C. Maria, G. Santos and T. Gunnlaugsson, *Dalton Trans.*, 2009, 4712; (d) J. T. Lin, Q. M. Wang, C. L. Tan and H. Y. Chen, *Synth. Met.*, 2010, **160**, 1780; (e) Q. M. Wang and Z. Zhou, *J. Sol-Gel Sci.Technol.*, 2011, **60**, 159.

20 (a) W. T. Xu, Y. F. Zhou, D. C. Huang, W. Xiong, M. Y. Su, K. Wang, S. Han and M. C. Hong, *Cryst. Growth Des.*, 2013, **13**, 5420; (b) W. T. Xu, Y. F. Zhou, D. C. Huang, M. Y. Su, K. W and M. C. Hong, *Inorg. Chem.*, 2014, **53**, 6497.

21(a) Y. M. Zhu, C. H. Zeng, T. S. Chu, H. M. Wang, Y. Y. Yang, Y. X. Tong, C. Y. Su and W. T. Wong, *J. Mater. Chem. A*, 2013, **1**, 11312; (b) W. Chen, S. Fukuzumi, *Inorg. Chem.*, 2009, **48**, 3800; (c) J. Y. Wu, T. T. Yeh, Y. S. Wen, J. Twu and K. L. Lu, *Cryst. Growth Des.*, 2006, **6**, 467.

22 (a) M. Shortreed, R. Kopelman, M. Kuhn, and B. Hoyland, *Anal. Chem.*, 1996, **68**, 1414; (b) W. Lin, L. Yuan, Z. Cao, Y. Feng and L. Long, *Chem. Eur. J*., 2009, **15**, 5096; (c) Y. Yang, T. Cheng, W. Zhu, Y. Xu and X. Qian, X. *Org. Lett*. 2011, **13**, 264; (d) M. Zhu, M. Yuan, X. Liu, J. Xu, J. Lv, C. Huang, H. Liu, Y. Li, S. Wang and D. Zhu, *Org. Lett.* 2008, **10**, 1481; (e) K. Tiwari, M. Mishra and V. P. Singh, *RSC Adv.*, 2013, **3**, 12124.

23 M. J. Frisch, G. W. Trucks, H. B. Schlegel, G. E. Scuseria, M. A. Robb, J. R. Cheeseman, G. Scalmani, V. Barone, B. Mennucci, G. A. Petersson, H. Nakatsuji, M. Caricato, X. Li, H. P. Hratchian, A. F. Izmaylov, J. Bloino, G. Zheng, J. L. Sonnenberg, M. Hada, M. Ehara, K. Toyota, R. Fukuda, J. Hasegawa, M. Ishida, T. Nakajima, Y. Honda, O. Kitao, H. Nakai, T. Vreven, J. A. Montgomery, Jr., J. E. Peralta, F. Ogliaro, M. Bearpark, J. J. Heyd, E. Brothers, K. N. Kudin, V. N. Staroverov, T. Keith, R. Kobayashi, J. Normand, K. Raghavachari, A. Rendell, J. C. Burant, S. S. Iyengar, J. Tomasi, M. Cossi, N. Rega, J. M. Millam, M. Klene, J. E. Knox, J. B. Cross, V. Bakken, C. Adamo, J. Jaramillo, R. Gomperts, R. E. Stratmann, O. Yazyev, A. J. Austin, R. Cammi, C. Pomelli, J. W. Ochterski, R. L. Martin, K. Morokuma, V. G. Zakrzewski, G. A. Voth, P. Salvador, J. J. Dannenberg, S. Dapprich, A. D. Daniels, O. Farkas, J. B. Foresman, J. V. Ortiz, J. Cioslowski and D. J. Fox, *Gaussian 09*, *revision D.01*.Gaussian, Inc., Wallingford CT, 2013.

24 (a) C. T. Lee, W. T. Yang and R. G. Parr, *Phys. Rev. B* 1988, **37**, 785; (b) A. D. Becke, *J. Chem. Phys.* 1993, **98**, 5648.

25 (a) M. Dolg, H. Stoll, A. Savin and H. Preuss, *Theor. Chim. Acta* 1989, **75**, 173; (b) M. Dolg, H. Stoll and H. Preuss, *Theor. Chim. Acta* 1993, **85**, 441.

26 S. Grimme, J. Antony, S. Ehrlich and H. Krieg, *J. Chem. Phys*., 2010, **132**, 154104.

27 (a) G. M. Sheldrick, *SHELXS-97, Program for solution of crystal structures*, University of Göttingen, Germany, 1997; (b) G. M. Sheldrick, *SHELXL-97, Program for refinement of crystal structures*, University of Göttingen, Germany, 1997.

28 (a) M. Fang, L. X. Chang, X. H. Liu, B. Zhao, Y. Zuo and Z. Chen, *Cryst. Growth Des.* 2009, **9**, 4006; (b) S. Q. Su, W. Chen, C. Qin, S. Y. Song, Z. Y. Guo, G. H. Li,; X. Z. Song, M. Zhu, S. Wang, Z. M. Hao and H. J. Zhang, *Cryst. Growth Des.* 2012, **12**, 1808.

29 A. Cabeza, M. A. G.Aranda and S.Bruque, *J. Mater. Chem.*, 1998, **8**, 2479.

30 (a) W. R. Fawcett and A. A. Kloss, *J. Phys. Chem.*, 1996, **100**, 2019; (b) F. A. Cotton, R. Francis, W. D. Horrocks, *J. Phys. Chem.*, 1960, **64**, 1534.

31 (a) R. Feng, F. L. Jiang, M. Y.Wu, L. Chen, C. F. Yan and M. C. Hong, *Cryst. Growth Des.*, 2010, **10**, 2306; (b) C. Yang, J. Xu, J. Ma, D. Zhu, Y. Zhang, L. Liang and M. Lu, *Polym. Chem.*, 2012, **3**, 2640.
32 (a) M. Kamiya and K. Johnsson, *Anal. Chem.*, 2010, **82**, 6472; (b)G. Zhang, N. Zhao, X. Hu and J. Tian, *Spectrochimica Acta Part A*, 2010, **76**, 410; (c) E. Gök, C. Öztürk and N. Akbay, *J. Fluoresc.*, 2008, **18**, 781; (d) Y. J. Hu, Y. Liu, J. B. Wang, X. H. Xiao and S. S. Qu, *J. Pharm. Biomed. Anal.*, 2004, **36**, 915.
33 D. F. Mullica, E. L. Sappenfield and L. A. Boatner, Inorg. *Chim. Acta.*, 1996, **244**, 247.
34 (a) A. Majjane, A. Chahine, M. Et-tabirou, B. Echchahed, T. Do and P. M. Breen, *Mater. Chem. Phys.*, 2014, **143**, 779; (b) Z. Chen, Q. Jin, Z. Guo, G. Montavon and W. Wu, *Chem. Eng. J.*, 2014, **256**, 61; (c) A. K. Fouchard, R.Drot, E. Simoni, N. Marmier, F. Fromage and J. J. Ehrhardt, *New. J. Chem.*, 2004, **28**, 864; (d) Q. H. Fan, X. L. Tan, J. X. Li, X. K. Wang, W. S. Wu, and G. Montavon, *Environ. Sci. Technol.*, 2009, **43**, 5776.
35 (a) G. R. J. Thatcher, D. R. Cameron, R. Nagelkerke and J. Schmitke, *J. CHEM. SOC., CHEM. COMMUN.*, 1992, 386; (b) M. Brynda, T. Wesolowski and K.Wojciechowski, *J. Phys. Chem. A*, 2004, **108**, 5091.
36 (a) Z. Liu, W. He and Z. Guo, *Chem.Soc.Rev.*, 2013, **42**, 1568; (b) Y. Bretonniere, M. J. Cann, D. Parker and R. Slater, *Org. Biomol. Chem.*, 2004, **2**, 1624; (c) Y. Bretonniere, M. J. Cann, D. Parker and R. Slater, *Chem. Commun.*, 2002, 1930.
37 O. Kotova, S. Comby and T. Gunnlaugsson, *Chem. Commun.*, 2011, **47**, 6810.
38 (a) H. Sigel, E. M. Bianchi, N. A. Corfu, Y. Kinjo, R. Tribolet and R. B. Martin, *Chem. Eur. J.*, 2001, **7**, 3729; (b) C. Grant, V. Frydman and L. Frydman, *J. Am. Chem. Soc.*, 2000, **122**, 11743; (c) S. Nadella, P. M. Selvakumar, E. Suresh, P. S. Subramanian, M. Albrecht, M. Giese and R. Fröhlich, *Chem. Eur. J.*, 2012, **18**, 16784.
39 (a) S. Mameri, L. J. Charbonnière and R. F. Ziessel, *Inorg. Chem.*, 2004, **43**, 1819; (b) X. Liu, J. Xu, Y. Lv, W. Wu, W. Liu and Y. Tang, *Dalton Trans.*, 2013, **42**, 9840; (c) E. A. Weitz, J. Y. Chang, A. H. Rosenfield and V. C. Pierre, *J. Am. Chem. Soc*., 2012, **134**, 16099; (d) S. Nadella, J. Sahoo, P. S. Subramanian, A. Sahu, S. Mishra and M. Albrecht, *Chem. Eur. J.*, 2014, **20**, 6047.

Table of contents entry

Eu_2PQC_6 has been developed to detect HSO_4^- and $H_2PO_4^-$ through different recognition mechanisms with low detection limits.